International Journal of Solids and Structures 50 (2013) 920–927

Contents lists available at SciVerse ScienceDirect

International Journal of Solids and Structures

journal homepage: www.elsevier.com/locate/ijsolstr

Crease in a ring of a pH-sensitive hydrogel swelling under constraint

Nicolas Zalachas [a], Shengqiang Cai [b], Zhigang Suo [b], Yuri Lapusta [a,*]

[a] French Institute of Advanced Mechanics, Institut Pascal/ UBP/CNRS/IFMA, Clermont Université, 63175 Aubière, France
[b] School of Engineering and Applied Sciences, Harvard University, Cambridge, MA 02138, USA

ARTICLE INFO

Article history:
Received 8 March 2012
Received in revised form 22 June 2012
Available online 5 December 2012

Keywords:
pH-sensitive gel
Large deformation
Finite element method
Crease instability

ABSTRACT

When a hydrogel swells, its surface often forms creases, a type of localized instability that nucleates and propagates in the form of self-contact. Motivated by recent applications of pH-sensitive hydrogels as actuators in adaptive lenses, here we analyze creases induced by constrained swelling. A ring of a gel, bonded between two rigid plates, swells by absorbing a solution from its external wall. The amount of swelling is adaptive in response to the change of the pH of the external solution. We analyze the large and inhomogeneous deformation in the gel by using a previously developed nonlinear field theory and finite element method. We show that, as the pH in the external solution increases, a short ring swells smoothly, but a tall ring forms a crease. We further show that the large deformation and instability can significantly affect the functionality of the adaptive lenses.

1. Introduction

A network of long polymer chains can imbibe a solution and swell, resulting in a gel. The amount of swelling is adaptive in response to changes in environmental stimuli. For example, acidic groups tethered to the polymer chains make the hydrogel adaptive to a change of pH value in the external solution. Such stimuli-responsive gels have been intensely developed as functional parts of many microsystems, including microfluidics (Beebe et al., 2000; Sugiura et al., 2007), micro-optics (Chang et al., 2010), and active surfaces (Tokarev and Minko, 2008). In the applications, gels swell under the constraint of hard materials, undergoing large deformation and instability.

This paper studies swelling and instability of pH-sensitive hydrogels. We are motivated by recent designs that use rings of hydrogels as actuators in microsystems (e.g. Dong et al., 2006; Dong and Jiang (2006); Zhu et al., 2011). A representative setup involves a ring of a pH-sensitive hydrogel bonded between two rigid plates (Fig. 1). A liquid immiscible with the hydrogel fills the space enclosed by the ring, while an aqueous solution containing mobile ions surrounds the ring. Another liquid is above of the top plate and is in contact with the liquid enclosed by the ring through a hole in the top plate. The interface of the two liquids forms a meniscus, which is used as a microlens. In response to a change of the pH value in the external solution, the ring absorbs or releases water. The deformation in the gel moves the liquid enclosed in the ring, changing the curvature of the meniscus and the focal length of the lens. A similar system has been designed with a ring of a temperature-responsive hydrogel (Dong et al., 2007; Zhu et al., 2011). Note that the human eye has an analogous way to achieve the function of focus by deforming the lens (Coleman, 1986).

Willis (1948) described the creasing instability in a compressed elastomeric tube. This instability has received theoretical and experimental studies (Dai and Wang, 2008; Beatty, 1987). In Willis's experiment, an elastomeric cylindrical tube is compressed with both ends fixed. When the compressive strain is relatively small, both inner surface and outer surface of the tube bulge outward to form convex surfaces. But with further the compression, a crease forms in the middle of the inner surface of the tube with a concave shape. We expect that similar instability may appear in the ring of the pH-sensitive hydrogel ring swelling under the constraint of the rigid plates.

Instabilities have been often observed in constrained swollen gels (e.g., Dervaux and Ben Amar, 2011; Trujillo et al., 2008; Tanaka et al., 1987). For example, during swelling, a free standing gel may swell inhomogenously in a short time and internal stresses are generated. The internal stresses can trigger different types of instability (e.g., Tanaka et al., 1987). After the gel is equilibrated with the solvent, there is no stress in the gel and the instability patterns disappear finally. However, if a gel swells under constraint, non-zero stresses can exist in an equilibrated gel. Therefore, instability has also been frequently observed in equilibrated constrained swollen gels (Dervaux and Ben Amar, 2011; Trujillo et al., 2008).

To analyze a variety of instability phenomena in gels, linear perturbation methods have been commonly adopted (e.g. Biot, 1965; Tanaka and Sigehuzi, 1993; Boudaoud and Chaieb, 2003). However, not all instabilities can be analyzed by the linear perturbation

* Corresponding author. Tel.: +33 4 73 28 80 49; fax: +33 4 73 28 81 00.
E-mail address: lapusta@ifma.fr (Y. Lapusta).

0020-7683/$ - see front matter © 2012 Elsevier Ltd. All rights reserved.
http://dx.doi.org/10.1016/j.ijsolstr.2012.11.015

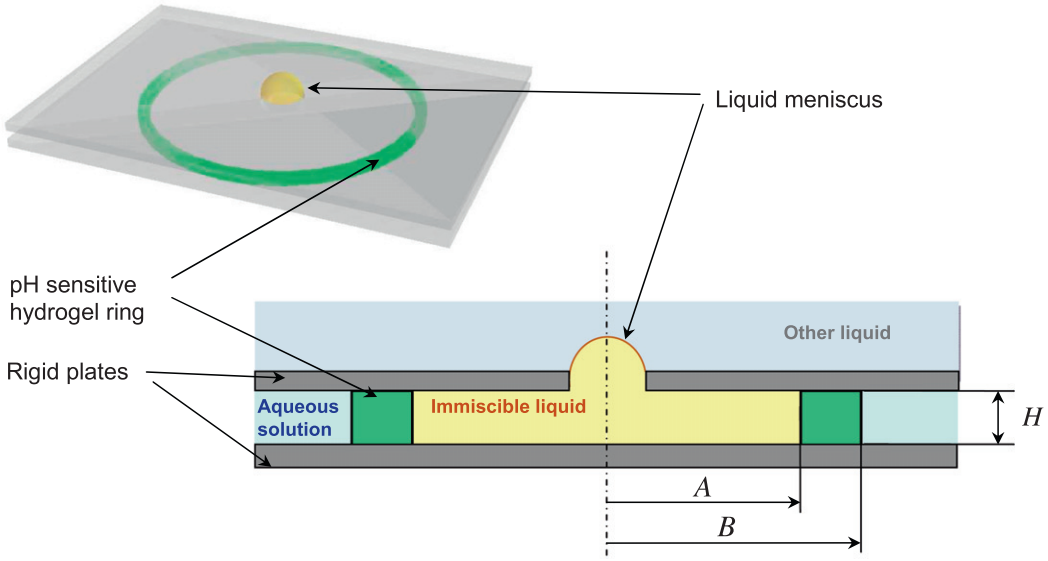

Fig. 1. Sketch of an adaptive liquid microlens, which is the meniscus between two liquids located in the center of the top surface. A ring of a pH-sensitive gel, height H, internal radius A and external radius B, is located between the top and bottom rigid plates. Outside the ring is an aqueous solution, and inside the ring is an immiscible liquid. A change in the pH of the external solution makes the ring deform and changes the focal length of the microlens.

method. In particular, the creasing instability cannot be analyzed by the linear perturbation method (Hohlfeld and Mahadevan, 2011; Hong et al., 2009a; Cai et al., 2012). In contrast to wrinkles, a crease is a nonlinear perturbation of the field of deformation which is localized in space. In Hong et al. (2009a), an energy method has been proposed to study the onset of creases in elastomers. In the study, energies in a creased and smoothly deformed body are calculated numerically. The energies of the two states are compared and the point of no difference in energies sets the critical condition of creasing instability (e.g. Wong et al., 2010; Kang and Huang, 2010; Cai et al., 2010; Hong et al., 2009a). Furthermore, Cai et al. (2012) find that the evolution of creasing instability can be fully analyzed numerically by introducing a small defect in the geometry with careful meshes. Although the creases have been frequently observed in constrained swollen gels (Trujillo et al., 2008; Kim et al., 2010; Yoon et al., 2010), the scientific study of creases in gels, especially the creases in stimuli-responsive hydrogels, is still in a nascent stage.

Here we focus on the large deformation behavior and the creasing instability in a ring of a pH-sensitive hydrogel swelling under the constraint of hard materials. Note that creases have never been calculated in pH-sensitive gels before, although they have been observed experimentally many times. Also, despite the existence of many experimental micro devices based on pH-sensitive gels, only very little work has been done to develop their numerical simulation in order to better understand these complex multi-physics phenomena. The new contribution of our work addresses directly these novel items of crease simulation in pH-sensitive gels and of modeling micro devices based on these materials. In this paper, the evolution of creasing in pH-sensitive gels is calculated for the first time. We use the field theory of a pH-sensitive hydrogel and the finite element method developed previously (Marcombe et al., 2010). As the pH value in the surrounding solution increases, the ring may undergo large deformation of two types (Fig. 2). When the ring is short, the ring swells smoothly and forms a barrel shape. When the ring is tall, a crease may develop on the internal surface of the ring. We further show that the large deformation and creasing instability can significantly affect the functionality of the adaptive microlens system.

2. Model description and theoretical background

2.1. Problem description

The theoretical system we study in this paper is illustrated in Fig. 1. A ring of a pH-sensitive hydrogel is located between two rigid horizontal plates. The ring is glued to the rigid plates. A liquid immiscible with the gel is inside the ring, while an aqueous solution is outside the ring. We assume that gel can only exchange solvent with the solution outside the ring, and the volume of immiscible liquid inside the ring keeps constant. A small circular hole in the center of the top plate makes the formation of a meniscus as the interface between two immiscible liquids. The meniscus is used as microlens in the experimental setup of Dong et al. (2006) described in the Introduction. The aqueous solution outside the ring is composed of solvent molecules, positive ions, negatives ions and hydrogen ions. A change in the pH in the external solution induces the deformation of the ring, which causes the change of the focal length of the liquid microlens.

To study the involved deformation of the gel ring quantitatively, we will use a nonlinear field theory of inhomogeneous deformation of pH-sensitive hydrogels and its finite element implementation (Marcombe et al., 2010). The theory focuses on the state of equilibrium at the long-time limit when the hydrogel has been in contact with the solution.

2.2. Equations of state of a pH-sensitive hydrogel

We first review the nonlinear field theory of a pH-sensitive hydrogel described in our previous paper (Marcombe et al., 2010). Consider a network of crosslinked polymers bearing acidic groups which is in equilibrium with an aqueous solution and mechanical forces (Fig. 3). The variation of the pH value in the external solution may cause the change of the amount of water in the gel. Let $\mathbf{X}$ be coordinate vector of a material particle of hydrogel in the state of a dry polymer, which is viewed as the reference state. When the hydrogel equilibrates with external solution and applied forces, the particle moves to a place with

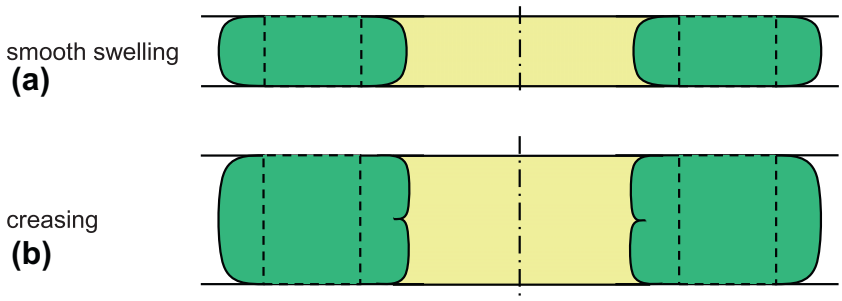

Fig. 2. Cross section of the deformed ring of the gel, which is bonded to the top and bottom plates. With the variation of the geometry, the ring may undergo two types of deformation: (a) smooth swelling and (b) creasing.

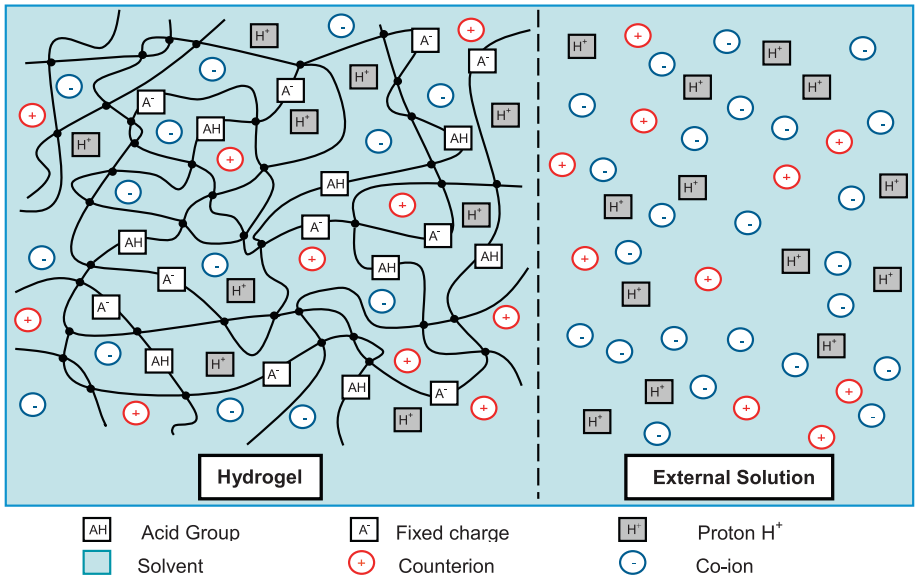

Fig. 3. pH-sensitive hydrogel is a polymer network that imbibes a solution. The polymer chains are covalently crosslinked and bear acidic groups AH. Some of the acidic groups dissociate into fixed charges attached to the network and mobile hydrogen ions in the solvent. Four mobile species are taken into account in the solution: solvent molecules, hydrogen ions, counterions and co-ions.

coordinate **x**, so, the field of deformation is fully described by the function $\mathbf{x} = \mathbf{x}(\mathbf{X})$. The deformation gradient of the network **F** is

$$F_{iK} = \frac{\partial x_i(\mathbf{X})}{\partial X_K} \tag{1}$$

In the external solution, let $\bar{n}_S, \bar{n}_-, \bar{n}_+$ and $\bar{n}_{H^+}$ be the number of solvent molecules, negative ions (co-ions), positive ions (counterions) and hydrogen ions. The electrochemical potential of corresponding species are denoted by μ_S, μ_-, μ_+ and μ_{H^+}. Define $dV(\mathbf{X})$ as an element of volume in the reference state, $dA(\mathbf{X})$ as an element of area in the reference state. In the current state, let $B_i(\mathbf{X})dV(\mathbf{X})$ be the external mechanical force applied on the element of volume and $T_i(\mathbf{X})\, dA(\mathbf{X})$ be the external mechanical force applied on the element of area.

The hydrogel, external solution and external forces constitute a thermodynamic system. The variation of the Helmholtz free energy of the system associated with small variation of $\mathbf{x}(\mathbf{X})$, $\bar{n}_S, \bar{n}_-, \bar{n}_+$ and $\bar{n}_{H^+}$, is equal to the sum of the variation of the free energy of the hydrogel $\int \delta W dV$, the free energy of external solution $\mu_S \delta\bar{n}_S + \mu_+ \delta\bar{n}_+ + \mu_- \delta\bar{n}_- + \mu_{H^+}\delta\bar{n}_{H^+}$ and the potential energy of the forces $\int B_i \delta x_i dV + \int T_i \delta x_i dA$. At a constant temperature, when the system is in equilibrium, the variation of free energy of the composite system is zero, namely,

$$\int \delta W dV + \mu_S \delta\bar{n}_S + \mu_{H^+}\delta\bar{n}_{H^+} + \mu_+ \delta\bar{n}_+ + \mu_- \delta\bar{n}_- - \int B_i \delta x_i dV - \int T_i \delta x_i dA = 0 \tag{2}$$

Define nominal concentration of a species in the gel as the number of the molecules divided by the volume of the hydrogel in the reference state, namely, the volume of the dry polymer. Denote $C_S(\mathbf{X}), \mathbf{C}_-(\mathbf{X}), \mathbf{C}_+(\mathbf{X})$ and $C_{H^+}(\mathbf{X})$ as the nominal concentrations of the solvent molecules, the co-ions, the counterions and the hydrogen ions respectively. The gel can only obtain the first three mobile species from the external solution, so we have the relation,

$$\int \delta C_\alpha(\mathbf{X}) dV + \delta\bar{n}_\alpha = 0 \qquad (\alpha = s, -, +). \tag{3}$$

The hydrogen ions in the gel can be either from the external solution or produced by the acidic group dissociation from the polymer chain. Indeed, as illustrated in Fig. 3, the hydrogel contains acidic groups-AH that may dissociate into fixed charges A^- attached to the network and the mobile hydrogen ions H^+. So, we have that,

$$\int \delta C_{H^+}(X) dV + \delta\bar{n}_{H^+} - \int \delta C_{A^-}(X) dV = 0 \tag{4}$$

Let f be the number of acidic groups AH attached to polymer network divided by the number of monomers in the network, and Ω be the volume per monomer. The sum of the number of the associated acidic groups AH and that of the fixed charges A^- equals the total number of the acidic groups:

$$C_{AH}(\mathbf{X}) + \mathbf{C}_{\mathbf{A}^-}(\mathbf{X}) = \mathbf{f}/\Omega. \tag{5}$$

Following the discussion in the previous paper (Marcombe et al., 2010), when the size of the gel is much larger than the Debye length, we can assume the electroneutrality of both the gel and the external solution, so that

$$C_{A^-}(\mathbf{X}) + \mathbf{C}_-(\mathbf{X}) = \mathbf{C}_{\mathbf{H}^+}(\mathbf{X}) + \mathbf{C}_+(\mathbf{X}) \tag{6}$$

$$\bar{n}_+ + \bar{n}_{H^+} = \bar{n}_-. \tag{7}$$

Considering the amount of the ions inside the gel is much smaller than the amount of water molecules in the gel, according to the molecular incompressibility assumption (Hong et al., 2009b), the total volume of the gel is equal to the sum of the volume of the dry polymer and the volume of the water,

$$1 + \Omega_s C_s = \det \mathbf{F} \tag{8}$$

where Ω_s is the volume of a single molecule of water.

Following the previous work (Marcombe et al., 2010), the free energy function of the pH sensitive hydrogel is assumed as the sum of the following contributions:

$$W = W_{net} + W_{sol} + W_{ion} + W_{dis}, \tag{9}$$

where W_{net} is the free energy of stretching of polymer network, W_{sol} is the free energy of mixing of polymer molecules with solvent, W_{ion} is the free energy of mixing ionic species with solvent and W_{dis} is the free energy of dissociation of weak acid. Eq. (9) describes an ideal elastomeric polyelectrolyte model, which is an extension of ideal elastomeric neutral gel model described in Cai and Suo (2012).

Next, we list the explicit function of each term in (9). The free energy related to the stretching of the network is described by the Gaussian-chain model:

$$W_{net} = \frac{NkT}{2}(F_{iK}F_{iK} - 3 - 2\log(\det \mathbf{F})), \tag{10}$$

where N is the number of polymer chains divided by the volume of the dry network, kT is the temperature in the unit of energy. The free energy of mixing the network and solvent is

$$W_{sol} = \frac{kT}{\Omega_S}\left[\Omega_S C_S \log\left(1 + \frac{1}{\Omega_S C_S}\right) + \frac{\chi}{1 + \Omega_S C_S}\right], \tag{11}$$

where χ is a dimensionless measured of the enthalpy of mixing. The free energy of mixing ionic species with solvent molecules is:

$$W_{ion} = kT\left[C_{H^+}\left(\log\left(\frac{C_{H^+}}{c^{ref}_{H^+}\det \mathbf{F}}\right) - 1\right) + C_+\left(\log\left(\frac{C_+}{c^{ref}_+ \det \mathbf{F}}\right) - 1\right) + C_-\left(\log\left(\frac{C_-}{c^{ref}_- \det \mathbf{F}}\right) - 1\right)\right] \tag{12}$$

where c^{ref}_α is a reference value of the concentration of a species. The free energy related to the dissociation of weak acid AH is:

$$W_{dis} = kT\left[C_{A-}\log\left(\frac{C_{A-}}{C_{A-} + C_{AH}}\right) + C_{AH}\log\left(\frac{C_{AH}}{C_{A-} + C_{AH}}\right)\right] + \gamma C_{A-}, \tag{13}$$

with γ enthalpy due to dissociation of acidic groups.The auxiliary conditions (3–8) reduce the number of independent fields that define the state of the swollen hydrogel to four, which can be $x_i(\mathbf{X}), C_-(\mathbf{X}), C_+(\mathbf{X})$ and $C_{H^+}(\mathbf{X})$. Therefore, the nominal density of free energy can be written as a function of four independent variables:

$$W = W(\mathbf{F}, C_+, C_-, C_{H^+}). \tag{14}$$

Let $\bar{c}_-, \bar{c}_+, \bar{c}_{H^+}$ be the true concentration of the three species of ions in the external solution. We assume that the external solution is dilute, so that the electrochemical potentials of the ions are,

$$\mu_+ - \mu_{H^+} = kT\log\left(\frac{\bar{c}_+ c^{ref}_{H^+}}{c^{ref}_+ \bar{c}_{H^+}}\right), \tag{15}$$

$$\mu_- + \mu_{H^+} = kT\log\left(\frac{\bar{c}_- \bar{c}_{H^+}}{c^{ref}_- c^{ref}_{H^+}}\right). \tag{16}$$

The chemical potential of water is taken to be,

$$\mu_S = -kT\Omega_S(\bar{c}_{H^+} + \bar{c}_+ + \bar{c}_-). \tag{17}$$

Inserting the explicit form of the free energy of the gel (9) into the condition of equilibrium (2) and combining all the equations above, we obtain the equations of state for a pH-sensitive hydrogel. Firstly, we can recover the condition of chemical equilibrium with respect to acidic dissociation,

$$K_a = \frac{C_{H^+}C_{A^-}}{C_{AH}N_A}, \tag{18}$$

with $N_A K_a = c^{ref}_{H^+}\exp(-\gamma/kT)$. We can also recover the conditions of Donnan equilibrium:

$$c_+/\bar{c}_+ = c_{H^+}/\bar{c}_{H^+}, \tag{19}$$

$$c_-/\bar{c}_- = (c_{H^+}/\bar{c}_{H^+})^{-1}. \tag{20}$$

The applied stress σ_{ij} equals the contractile stress of the network minus the osmotic pressure

$$\sigma_{ij} = \frac{NkT}{\det \mathbf{F}}(F_{iK}F_{jK} - \delta_{ij}) - (\Pi_{sol} + \Pi_{ion})\delta_{ij} \tag{21}$$

where,

$$\Pi_{ion} = kT(c_{H^+} + c_+ + c_- - \bar{c}_{H^+} - \bar{c}_+ - \bar{c}_-), \tag{22}$$

$$\Pi_{sol} = -\frac{kT}{\Omega_S}\left\{\log\left(1 - \frac{1}{\det \mathbf{F}}\right) + \frac{1}{\det \mathbf{F}} + \frac{\chi}{(\det \mathbf{F})^2}\right\}. \tag{23}$$

Π_{ion} is the osmotic pressure due to the imbalance of the number of ions in the gel and in the external solution, and Π_{sol} is the osmotic pressure due to mixing the network and the solvent.

2.3. Finite element implementation

The variational statement (2) for inhomogeneous swelling of the pH-sensitive hydrogel can be transformed to the format commonly used in finite element analysis. This is realized by using the Legendre transformation of the free energy function:

$$\hat{W} = W - (\mu_+ - \mu_{H^+})C_+ - (\mu_- + \mu_{H^+})C_- - \mu_S C_S. \tag{24}$$

Inserting the above equation into (2), with auxiliary conditions (3–8), we have that

$$\int \delta\hat{W}dV = \int B_i\delta x_i dV + \int T_i\delta x_i dA, \tag{25}$$

where $\hat{W}$ is a new free energy of the pH-sensitive gels, which can be directly implemented into most finite element analysis programs.

Note that taking into account chemical equilibrium (18), Donnan equilibrium (19) and (20), the new free energy function depends only on the deformation gradient and the concentrations of positive ions and hydrogen ions in the external solution:

$$\hat{W} = \hat{W}(\mathbf{F}, \bar{c}_{H^+}, \bar{c}_+). \tag{26}$$

The free energy function has been implemented by Marcombe et al. (2010) into a subroutine UHYPER in ABAQUS.

3. Numerical simulations and discussions

3.1. Numerical simulation of creasing instabilities in a pH-sensitive gel

To analyze both the onset and subsequent development of creases, we use the commercial finite-element software ABAQUS with implemented user-subroutine for pH-sensitive gels. The deformation in the ring, which is glued to the rigid plates, is assumed to be axisymmetric. 8-node biquadratic axisymmetric quadrilateral, hybrid reduced integration element (CAX8RH) is used in the numerical simulations. Since a crease will emerge wherever the strain first exceeds the critical value, only a small perturbation (defect) is necessary to break translational invariance and specify the position of the crease. The small perturbation is introduced by placing in the finite element mesh a defect—a quarter of a circle of a small radius. Note that a defect of any reasonable shape and size would generate a crease provided that it is sharp enough to concentrate strains at its tip. We chose the quarter of circle because this shape allows smooth geometry transitions without corners and improves the convergence of calculation. To eliminate the effect of the size of the defect, the defect is made much smaller than the characteristic length, thickness of the ring, $B - A$. To resolve the field close to the tip of the crease, the defect is made much larger than the size of the finite elements around the defect. Note that this method works well to generate creases, see e.g. previous work on elastomers Hong et al. (2009a), Cai et al. (2010) and Cai et al. (2012). The perturbation is introduced in the middle of the inner surface of the ring (Fig. 4). This choice of the defect location is dictated by the following considerations. Firstly, Willis' (1948) observations for hollow rubber cylinders confirm clearly that a crease generates at this location and not elsewhere. Secondly, the location where a crease is expected and, thus, where a defect is included has to attain the critical compressive strain for a crease to generate. Only when the critical compressive strain is locally reached, the crease nucleates and propagates. Our numerical calculation without defect indicates clearly the highest compressive strain located in the middle of the inner side of the ring, which, along with the Willis experiment, confirms our assumption. Recall that, to obtain the solution near the crease tip, the size of the finite elements around the defect is made much smaller than the size of the defect. The surface of the ring is allowed to fold and self-contact. Following Marcombe et al. (2010), we use the following dimensionless parameters for the pH-sensitive hydrogel in the calculations: $N\Omega_s = 0.001, \chi = 0.1, \mathrm{pK}_a = 4.25$ and $f = 0.1$. To simplify the calculations, the volume per monomer is assumed to equal the volume per solvent molecule, namely $\Omega = \Omega_s$. We further assume that the pH-sensitive gel ring is stress free when the pH in the external solution is $\overline{\mathrm{pH}}_0 = 2$ and the concentration of positive ions is $C_0 = 0.001$ M.

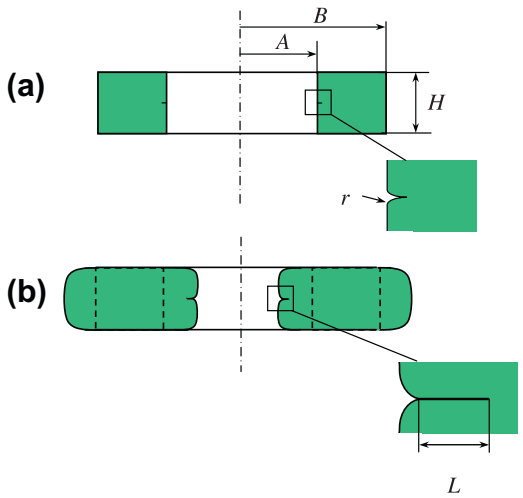

Fig. 4. The schematic of the numerical simulation of the creasing instability in the ring of the gel. (a) A small defect is introduced in the middle of the inner surface. (b) When the gel swells, self-contact may propagate. $B/A = 1.5$ is fixed in all the calculations, but H/A is varied.

3.2. Results and discussions

Results of simulations provided in Fig. 5 illustrate the behavior of rings of the pH-sensitive gel of different heights H/A and the fixed $B/A = 1.5$. When $H/A < 0.56$, the ring swells smoothly, developing a barrel shape in the whole range of pH values (Fig. 5a), and the inner surface of the hydrogel ring is convex. When $H/A > 0.56$, the ring swells smoothly for a limited range of pH value and a crease develops on the inner surface (Fig. 5b–d). The depth of the crease can be as large as one fifth of the thickness of the ring. Our simulation results for the constrained swollen pH-sensitive qualitatively agree with the observations in Willis experiments summarized in the Introduction. In applications, cyclic formation of creases at the inner surface of the gel ring may initiate a premature failure of the system.

The nucleation and growth of a crease can be represented by plotting the depth of the crease as a function of the pH (Fig. 6). When $H/A < 0.56$, no self-contact develops for the whole calculated range of pH. When $H/A = 0.56$, a self-contact zone starts to initiate when the pH value is around pKa = 4.25, but then disappears when the pH value becomes large. When $H/A > 0.56$, the length of the self-contact zone increases significantly when the pH value is above pKa = 4.25 of the gel system. Therefore, $H/A = 0.56$ is approximately a boundary between smooth deformation and creasing. Fig. 6b shows the growth of the self-contact zone of the gel ring with increasing the pH value for several large values of H/A. After an abrupt increase, the self-contact length of the gel ring can reach a significant portion of the ring thickness. When the pH value is the same in the external solution, larger self-contact zone develops with larger value of H/A. For example, when pH = 10 for the gel ring with $H/A = 0.59$, the self-contact length reaches about 15% of the thickness of the ring. When pH = 10 for the gel ring with $H/A = 1.5$, the self-contact length can reach 50% of the thickness of the ring. It is important to note that, in the simulations with $H/A > 0.56$, the introduction of a small defect on the inner surface of the gel ring helps significantly the calculations to converge. If no defect is introduced, the calculation often stops when the crease is supposed to initiate. We interpret this stop in finite element calculation as another sign of the instability.

For the particular application illustrated in Fig. 1, the volume enclosed by the ring and the rigid plates is directly related to the focus length of the liquid microlens. Fig. 7 plots the change of the enclosed volume as a function of pH value. The difference between the current and initial volume is normalized by the initial volume. The aspect ratio H/A can have a significant influence on the volume change, and, hence, on the functionality of the lens. The relative volume change can be both positive and negative, depending on the aspect ratio H/A. For our calculated geometries, the negative volume change can be as large as 50% of the initial volume and the positive volume change can be as large as 1.5 times the initial volume. Understanding of this behavior is of crucial importance for the design of the adaptive liquid lens considered in Fig. 1.

According to our results, it is possible to vary the value H/A in such a way that it determines the types of lens upon increasing

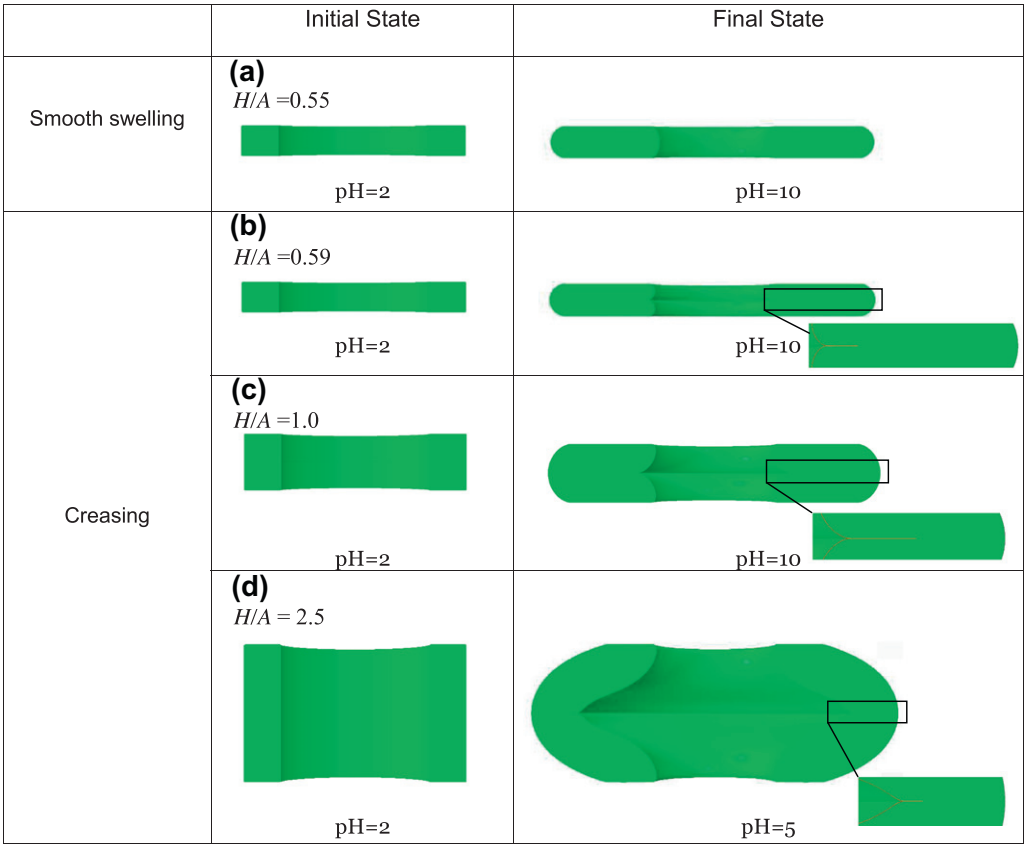

Fig. 5. Results of simulations. Initial and final states of the pH sensitive gel ring with different values of aspect ratio H/A. (a) The ring swells smoothly pH = 10. (b) The ring swells smoothly for small pH value, while self-contact begin to propagate at the inner surface to form a crease when pH becomes bigger. (c and d) Concavity is enhanced as aspect ratio increases. The outer surface swells and self contact develops in the center of the inner surface. (d) The ring collapses at a smaller value of pH = 5. Close-up views on the right show the crease at final state. The region of small values of H/A corresponds to the smooth swelling for any values of pH. The region of bigger values of H/A corresponds to unstable swelling where creasing propagates with increasing pH. Transition from smooth swelling to creasing occurs around the approximate value $H/A = 0.56$. Note that this condition is satisfied for the dimensions of the adaptive optics device described in Dong et al., 2006.

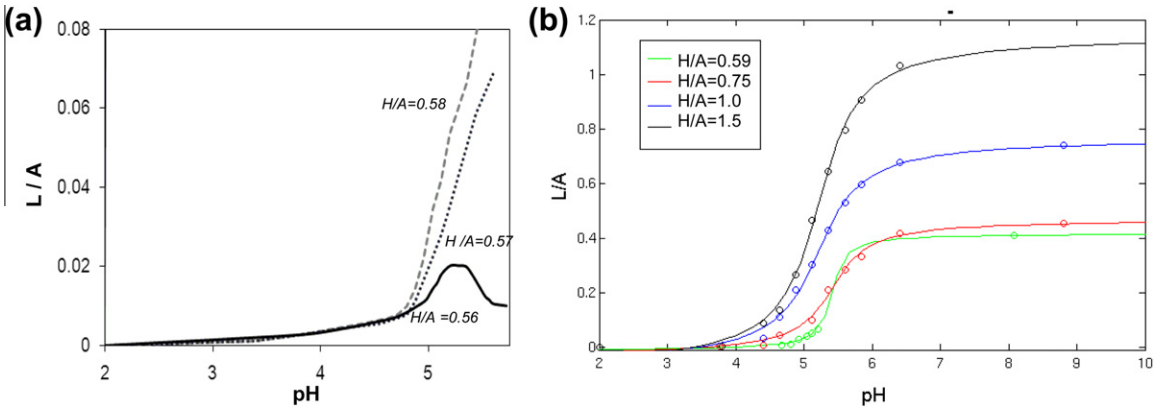

Fig. 6. Normalized crease depth L/A versus pH for several aspect ratios H/A. (a) For small values of H/A, only smooth swelling occurs and no crease propagates. At around $H/A = 0.56$, a transition between smooth swelling and creasing happens. Self-contact sets in first and reduces around pH = 5. (b) For larger values of H/A, the crease propagates. For example, when $H/A = 0.59$, the self-contact length increases with pH and finally saturates at high pH values. Small circles represent the discrete results obtained from finite element simulations.

pH value in the solution. We consider the refractive index of the liquid above larger than that of immiscible liquid inside the ring. The meniscus bulged upward diverges incident light from the bottom of the structure and the one bulged downward converges light. We consider an initial meniscus that is bulged upward as in Fig. 1. When $H/A < 1$, the inner liquid pushes the meniscus up with increasing the pH value, keeping in that case a divergent lens for the incident light from the bottom. This case corresponds to the application principle of the adaptive optics device reported in the Fig. 3 from Dong et al. (2006). When $H/A > 1$ and with the same initial curvature of the liquid lens, an increasing of pH makes the inner surface of the ring bulge outward in the radial plane. The meniscus is sucked down and the liquid lens becomes convergent for the incident light from the bottom. For even larger values of $H/$

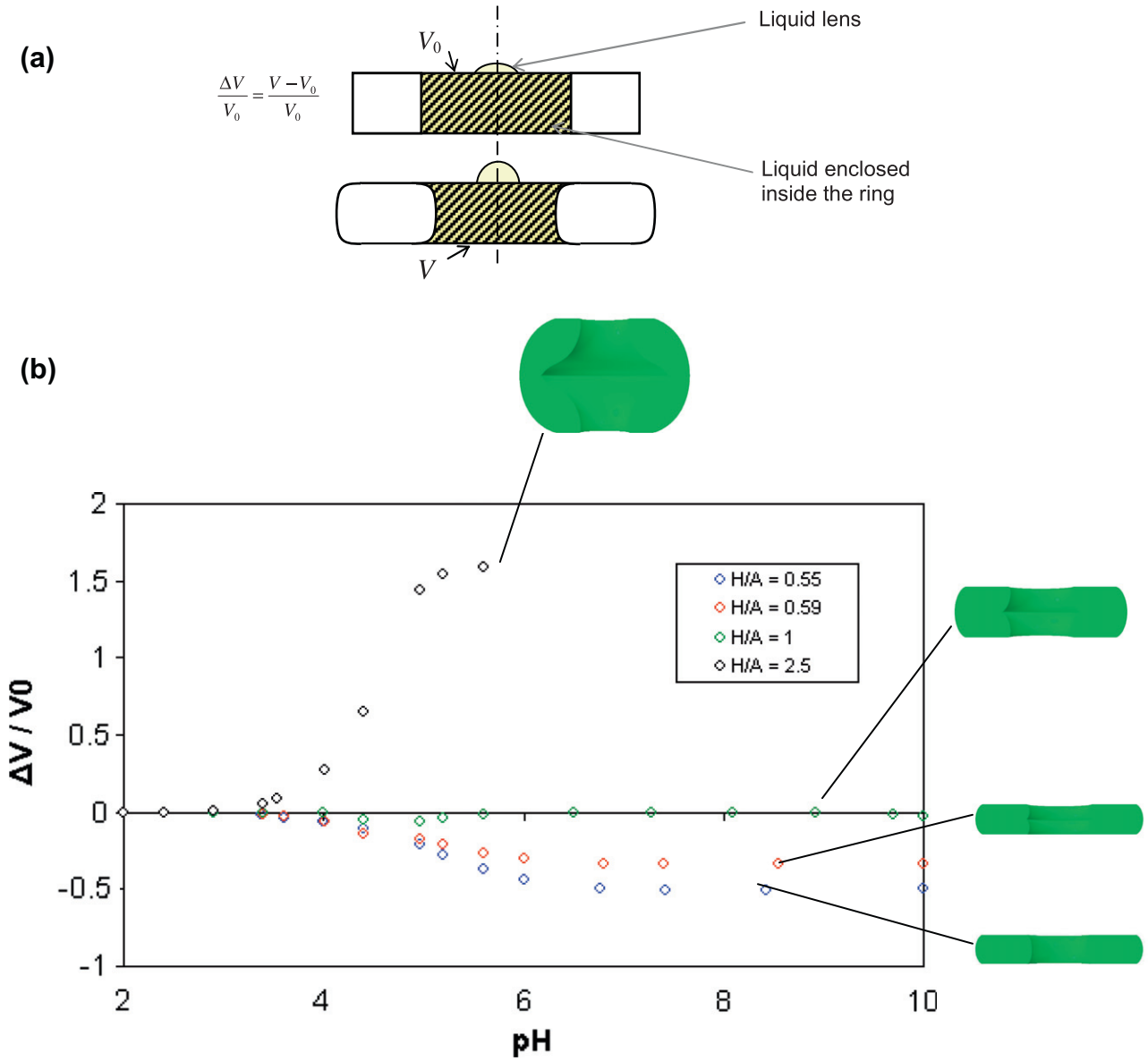

Fig. 7. Change in the volume enclosed by the ring ΔV, normalized by the initial volume. Volumes V_0 is plotted as a function of pH for several different aspect ratios H/A. (a) The calculated volume is shaded. (b) The variation of volume becomes negative when H/A is smaller than 1. In the calculated range of the aspect ratio H/A, the negative volume change can reach 50% for $H/A = 0.55$, while the positive volume change can reach 150% for $H/A = 2.5$.

A, one could also take advantage of the creasing instability, under assumption that it does not make the ring collapse. For instance, the large amount of negative volume change for high values of H/A (around $H/A = 2$) would be useful to drive the focus lens of a larger liquid meniscus.

A direct comparison between our calculations and experimental results from Dong et al. (2006) is difficult at this writing due to the lack of experimental measurements (e.g., deformed shapes of the ring, material properties of the AA hydrogel). Moreover, compared to the original experimental setup of Dong et al. (2006), our calculation models made some modifications. For example, in our model, we assume that the liquid enclosed by the ring is immiscible and cannot be absorbed by the gel. The gel can only exchange solvent molecules with the solution outside the gel ring. The volume of the liquid inside the gel ring is conserved, which enables a reliable control of the micro-optics system, namely, the focus length of the liquid meniscus. In the system described in Dong et al. (2006), the liquid enclosed by the gel ring is also an aqueous solution. Therefore, the solution already absorbed by the gel can exchange with the solution enclosed by the ring via osmosis. Consequently the volume of liquid enclosed by the gel ring may not be conserved in such a system. Furthermore, because the gel is permeable to the aqueous solution outside, the solvent enclosed by the gel ring will transport through the gel to equilibrate with the aqueous solution outside. Therefore, some of the behaviors observed in the experiments of Dong et al. (2006) may be transient. In addition, due to the complexity of the whole solvent exchanges, the structure becomes less controllable and predictable. Last, in our model we assume the ring is glued to the rigid plates. This does not allow the gel ring to move. That may not be the real setup in the experiment from Dong et al. (2006), where the ring of hydrogel is constructed by photopaterning prepolymer mixtures.

4. Conclusion

We have analyzed large-deformation swelling and creasing instability in a constrained swollen ring of a pH sensitive hydrogel. Depending on the height of the ring, the system behaves very dif-

ferently. When the ring is short, a smooth barrel-shaped swelling develops in the ring in a wide range of pH values. The inner surface of the hydrogel ring becomes convex. When the ring is tall, the ring swells smoothly only for small pH values. As the pH further increases, a crease appears and a self-contact develops and propagates. The inner surface of the hydrogel ring can even become concave for higher values of aspect ratio H/A. We further illustrate that the deformation type in the ring may have a very significant influence on the performance of the liquid adaptive lens system. We hope that our computational method will aid the development of adaptive systems using stimuli-responsive hydrogels.

Acknowledgments

The work at Harvard is supported by ARO (W911NF-09-1-0476), DARPA (W911NF-10-1-0113), and MRSEC. The work at the Institut Pascal and IFMA is supported by Laboratoire d'excellence IMobS^3.

References

Beatty, M., 1987. Topics in finite elasticity: hyperelasticity of rubber, elastomers, and biological tissues – with examples. Appl. Mech. Rev. 40, 1699–1734.

Beebe, D.J., Moore, J.S., Bauer, J.M., Yu, Q., Liu, R.H., Devadoss, C., Jo, B.H., 2000. Functional hydrogel structures for autonomous flow control inside microfluidic channels. Nature 404, 588–590.

Biot, M.A., 1965. Mechanics of Incremental Deformation. Wiley, New York.

Boudaoud, A., Chaieb, S., 2003. Mechanical phase diagram of shrinking cylindrical gels. Phys. Rev. E 68, 021801.

Cai, S.Q., Bertoldi, K., Wang, H.M., Suo, Z.G., 2010. Osmotic collapse of a void in an elastomer: breathing, buckling and creasing. Soft Matter 6, 5770–5777.

Cai, S.Q., Chen, D.Y., Suo, Z.G., Hayward, R.C., 2012. Creasing instability of elastomer films. Soft Matter 8, 1301–1304.

Cai, S.Q., Suo, Z.G., 2012. Equations of state for ideal elastomeric gels. EPL 97, 34009.

Chang, C.L., Ding, Z.W., Patchigolla, V.N.R., Ziaie, B., Savran, C.A., 2010. Diffractometric biochemical sensing with smart hydrogels. IEEE Sens., 1617–1621.

Coleman, J., 1986. On the hydraulic suspension theory of accommodation. Tr. Am. Ophthalmol. Soc. 84, 846–868.

Dai, H., Wang, F., 2008. Bifurcation to a corner-like formation in a slender nonlinearly elastic cylinder: asymptotic solution and mechanism. Proc. R. Soc. A. 464, 1587–1613.

Dervaux, J., Ben Amar, M., 2011. Buckling condensation in constrained growth. J. Mech. Phys. Solids 59, 538–560.

Dong, L., Agarwal, A.K., Beebe, D.J., Jiang, H.R., 2007. Variable-focus liquid microlenses and micolens arrays actuated by thermoresponsive hydrogels. Adv. Mater. 19, 401–405.

Dong, L., Agarwal, A.K., Beebe, D.J., Jiang, H.R., 2006. Adaptive liquid microlenses activated by stimuli responsive hydrogels. Nature 442, 551–554.

Dong, L., Jiang, H.R., 2006. PH-adaptive microlenses using pinned liquid-liquid interfaces actuated by pH-responsive hydrogel. Appl. Phys. Lett. 89, 211120.

Hohlfeld, E., Mahadevan, L., 2011. Unfolding the sulcus. Phys. Rev. Lett. 106, 105702.

Hong, W., Zhao, X.H., Suo, Z.G., 2009a. Formation of creases on the surfaces of elastomers and gels. Appl. Phys. Lett. 95, 111901.

Hong, W., Liu, Z.S., Suo, Z.G., 2009b. Inhomogeneous swelling of a gel in equilibrium with a solvent and mechanical load. Int. J. Solids Struct. 46, 3282.

Kang, M.K., Huang, R., 2010. A variational approach and finite element implementation for swelling of polymeric hydrogels under geometric constraints. J. Appl. Mech. 77, 061004.

Kim, J., Yoon, J., Hayward, R., 2010. Dynamic display of biomolecular patterns through an elastic creasing instability of stimuli-responsive hydrogels. Nat. Mater. 9, 159–164.

Marcombe, R., Cai, S.Q., Hong, W., Zhao, X.H., Lapusta, Y., Suo, Z.G., 2010. A theory of constrained swelling of a pH-sensitive hydrogel. Soft Matter 6, 784–793.

Sugiura, S., Sumaru, K., Ohi, K., Hiroki, K., Takagi, T., Kanamori, T., 2007. Photoresponsive polymer gel microvalves controlled by local light irradiation. Sens. Actuators A 140, 176–184.

Tanaka, H., Sigehuzi, T., 1993. Surface-pattern evolution in a swelling gel under a geometrical constraint: direct observation of fold structure and its coarsening dynamics. Phys. Rev. E 49, R39–R42.

Tanaka, T., Sun, S.T., Hirokawa, Y., Katayama, S., Kucera, J., Hirose, Y., Amiya, T., 1987. Mechanical instability of gels at the phase transition. Nature 325, 796–798.

Tokarev, I., Minko, S., 2008. Stimuli-responsive hydrogel thin films. Soft Matter 5, 511–524.

Trujillo, V., Kim, J., Hayward, R., 2008. Creasing instability of surface-attached hydrogels. Soft Matter 4, 564–569.

Willis, A.H., 1948. Instability in hollow rubber cylinders subjected to axial loading. In: VII International Congress of Applied Mechanics, pp. 280–296.

Wong, W.H., Guo, T.F., Zhang, Y.W., Cheng, L., 2010. Surface instability maps for soft materials. Soft Matter 6, 5743–5750.

Yoon, J., Kim, J., Hayward, R., 2010. Nucleation, growth and hysteresis of surface creases on swelled polymer gels. Soft Matter 6, 5807–5816.

Zhu, D.F., Zeng, X.F., Li, C.H., Jiang, H.G., 2011. Focus-tunable microlens arrays fabricated on spherical surfaces. J. Microelectromech. Sys. 20, 369–395.